EURASIAN PHYSICAL TECHNICAL JOURNAL

2024, Volume 21, No. 4(50)

https://doi.org/10.31489/2024No4/49-60

Received: 24/06/2024 Revised: 10/08/2024 Accepted: 17/12/2024 Published online: 25/12/2024

Original Research Article

UDC 536.8

SIMULATION OF CONDITIONS FOR ACHIEVING HIGH ELECTRICAL POWER AND EFFICIENCY IN A STIRLING ENGINE WITH A FREE WORKING PISTON

Sabdenov K. O.[1]*, Erzada M.[1], Zholdybaeva G.T.[2]

[1] L.N. Gumilyov Eurasian National University, Astana, Kazakhstan

[2] M. Saparbaev South Kazakhstan Humanitarian Institute, Shymkent, Kazakhstan

Corresponding author: sabdenovko@yandex.kz

Abstract. *A simulation of the Stirling engine was carried out, where the temperature variability in the cooler and heater is taken into account, and the engine itself generates electric current. The study was carried out in the temperature range when the piston and displacer move synchronously. The possibility of increasing engine power by reducing hydraulic resistance in the regenerator is shown. It was also discovered that as the electrical load on the generator increases, the work produced by the engine can also increase. This indicates that there is a maximum of electrical energy production depending on the load. The increased rigidity of the displacer spring contributes to an increase in engine power and its efficiency.*

Keywords: free-piston Stirling engine, regenerator, displacer, efficiency.

1. Introduction

Due to the limited reserves of oil, gas and high-quality coal on the planet, the problem of energy shortages will arise in the near future. Therefore, new thermodynamic cycles and the possibility of creating heat engines based on them are being sought [1–4]. In this context, the Stirling engine deserves attention; it unites a large family of devices whose operation is based approximately on the thermodynamic Stirling cycle [5, 6]. It belongs to a wide class of low-power motors for producing mechanical work and/or electrical energy from low-potential heat sources [7–11]. Based on the Stirling engine, it is possible to create an energy system with distributed generation [12, 13]. This is important for Kazakhstan, which has a low population density and rich solar energy resources. Mathematical modeling of the Stirling engine makes it relatively easy to find the most important conditions and parameters necessary to create devices with the highest efficiency.

Widely used isothermal models [1–3, 6, 13–15] have low accuracy and are not convenient for designing real Stirling engines, although they allow us to understand their basic properties. Therefore, a model is needed that takes into account the temperature change in all parts of the engine, since the temperature changes greatly and this factor can have a significant impact on the physical characteristics of the designed devices.

In addition, there is another important question about the role of spring 4 (Fig. 1) in the engine operation. The fact is that the Stirling engine can operate without this spring, and no separate studies devoted to its influence on such important characteristics as power and efficiency can be found.

The proposed work analyzes the operation of a Stirling engine with a free working piston; in contrast to earlier works, the temperature variability in the heater and cooler is taken into account. This is very

important, since widespread isothermal models [1–3, 7, 14, 15] are not convenient for designing real engines, although they allow one to understand their basic properties.

An attempt to take into account the temperature variability in work [14] does not solve the problem, since it uses approximate equations that are valid only for the steady-state heat exchange mode. The same is done in [1-3, 6]. It is not possible to find other studies that describe in detail the temperature change over time in a Stirling engine. In addition, the proposed study, unlike [1-3, 6, 14], is based on a simpler and at the same time more advanced model [13]; in it, the engine is considered to consist of three parts (instead of five) — a heater, cooler and regenerator. There is another difference: a non-stationary equation of conservation of momentum is used for the regenerator. This equation more accurately takes into account the momentum transfer in the regenerator and, for a steady gas flow, goes over to the Darcy-Weisbach equation from works [1-3, 6, 14].

2. Engine design diagram and model equations

In Fig. 1 shows a diagram of the design of a Stirling machine with a free piston [14, 15]. Compression volume 6 is a cooler and is designated V_c, expansion volume 7 is a heater with volume V_e. This means that the volumes V_c and V_e are essentially a cooler and a heater, they are cylindrical in shape with a diameter d_2. Accordingly, their temperatures are T_c and T_e. Volumes V_c and V_e are in contact with "external environments" with minimum $T_{\min}$ and maximum $T_{\max}$ temperatures. The gas masses in each of the indicated volumes are equal to m_c and m_e.

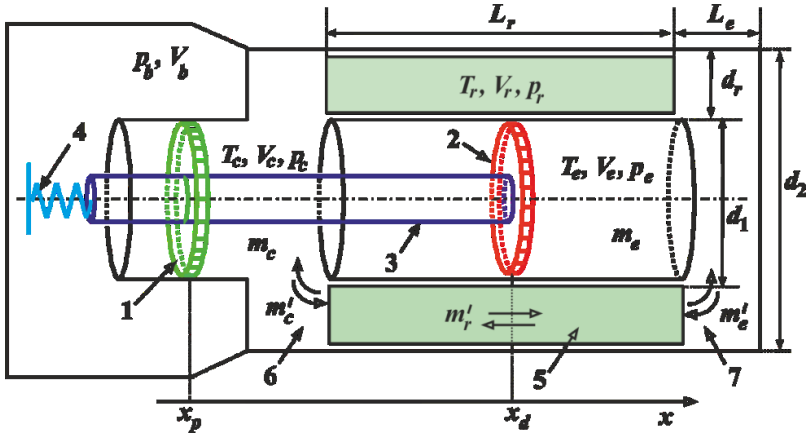

Fig. 1. Simplified diagram of the structure of a Stirling engine with a free piston and the direction of the x coordinate: 1 – working piston; 2 – displacer; 3 – displacer rod; 4 – displacer spring; 5 – regenerator; 6 – cooling area; 7 – heating area

The origin of coordinates x coincides with the initial position of the working piston when it is in the equilibrium position $x_p = 0$. This state corresponds to the initial position of the displacer $x_d = x_{d,0}$. Regenerator 5 is a narrow and long channel in the space between two coaxial cylinders with diameters d_1 and $d_2 = d_1 + 2d_r$. In it, gas moves in the direction of coordinate x with a cross-sectional average speed u and density ρ_r. The buffer space includes volume V_b, pressure p_b in it, according to the results of [15], it does not play a big role.

The displacer and the working piston have the shape of a disk of equal diameter d_1. The working piston 1 moves freely along the rod 3 of the displacer 2, the last two are rigidly connected to each other, and one of the ends of the rod is attached to the spring 4 with a stiffness coefficient k_d. The displacer can move freely inside the cylinder, surrounded by a cylindrical regenerator with length L_r and working space thickness d_r. When the piston moves, an electric current is generated, the linear generator in Fig. 1 is not shown, but its reverse effect on the operation of the machine is taken into account by the damping coefficient D_p [14].

A new isothermal model of the engine is presented in [15], it includes the equations of motion of the displacer, piston and gas in the regenerator, and takes into account the relaxation property of the regenerator of a hydrodynamic nature. The coordinate of the displacer x_d with mass m_d is measured from the equilibrium position $x_{d,0}$, the initial state of the piston coordinate x_p and mass m_p coincides with the x coordinate. The gas

in the buffer volume compresses and expands under adiabatic conditions with index γ. External and initial pressure p_0. The equations of motion of the displacer and piston have the form

$$m_d \frac{d^2 x_d}{dt^2} + k_d (x_d - x_{d,0}) = p_b A_{rod} + p_c A_p - p_e A_d, \tag{1}$$

$$m_p \frac{d^2 x_p}{dt^2} + D_p \frac{dx_p}{dt} = (p_b - p_c) A_p. \tag{2}$$

They are supplemented by formulas for determining pressures:

$$p_b = p_0 \left(\frac{V_{b,0}}{V_b} \right)^{\gamma}, \qquad p_c = \frac{R_g T_c}{V_c} m_c, \qquad p_e = \frac{R_g T_e}{V_e} m_e. \tag{3}$$

The volumes contained here are found by the equations

$$V_c = V_{c,0} + A_p (x_d - x_{d,0} - x_p), \qquad V_e = V_{e,0} - A_d (x_d - x_{d,0}), \tag{4}$$

$$V_{e,0} = X_{e,0} \frac{\pi d_1^2}{4} + L_e \frac{\pi d_2^2}{4}, \quad V_b = V_{b,0} + A_{rod} (x_d - x_{d,0}) + A_p x_p.$$

Here $X_{e,0}$ is the distance from the right wall of the heater to the equilibrium position of the displacer; A_{rod} is the cross-sectional area of rod of the displacer; A_d is the cross-sectional area of the displacer, and $A_d = \pi d_1^2 / 4$.

In equations (1) and (2) there are no reaction forces from the walls that arise when the piston and displacer reach the extreme positions on the left $x_{d,\min}$, $x_{p,\min}$ and on the right $x_{d,\max}$, $x_{p,\max}$. In this study, only such operating modes are considered when such values of the coordinates of the piston and displacer are not achieved. The gas masses in the displacer m_c and heater m_e are determined by solving the equations (further, the top stroke means the derivative with respect to time)

$$\frac{dm_c}{dt} = -m_r', \quad \frac{dm_e}{dt} = m_r'. \tag{5}$$

Let $m_{c,0}$ and $m_{e,0}$ are the initial values of the gas masses in the cooler and heater, then from the sum of equations (5) and after integration the equality follows

$$m_c - m_{c,0} = -(m_e - m_{e,0}). \tag{6}$$

The pressure p_r and temperature T_r in the regenerator are taken to be the average values in the heater and cooler:

$$p_r = \frac{p_e + p_c}{2}, \quad T_r = \frac{T_e + T_c}{2}. \tag{7}$$

Equalities (7) mean accepting a linear dependence on the x coordinate of changes in pressure and temperature in the regenerator. Then the average gas density in the regenerator ρ_r is determined from the equation of state

$$\rho_r = \frac{p_e + p_c}{(T_e + T_c) R_g}. \tag{8}$$

For the gas mass flow rate in the regenerator $m'_r(t) = u(t)\rho_r A_r$, the equation is used [15]

$$\frac{dm_r'}{dt} = \frac{A_r}{L_r} \Delta p - \frac{1}{2} \frac{K_\Sigma |m_r'|}{m_r} m_r', \tag{9}$$

$$K_\Sigma = K_r + \frac{L_r}{2 d_r} \zeta, \quad m_r = \rho_r L_r A_r = \rho_r V_r, \quad V_r = L_r A_r. \tag{10}$$

According to the diagram in Fig. 1, the positive direction of gas movement corresponds to the positive sign of the pressure drop Δp, therefore $\Delta p = p_c - p_e$.

Writing the energy equation comes down to finding an equation for the temperature of the heater T_e and cooler T_c; these parts of the machine are surrounded by media with temperatures $T_{\max}$ and $T_{\min}$. In real devices, $T_{\max}$ is the temperature of the liquid or gaseous medium that serves as a heat supplier for the machine; $T_{\min}$ is the ambient temperature.

Heat exchange with the external environment occurs according to Newton's law with heat transfer coefficients α_e and α_c through the wall surfaces with the contact area S_e and S_c. Using Newton's law does not accurately model heat transfer through the wall during fast transient processes, but is acceptable as a first approximation.

The heat capacity of a gas at a constant volume c_υ = const, the mass of the gas m, the internal energy of the gas $U = c_\upsilon mT$, when a small heat dQ is supplied, its volume changes by the value dV, then the law of conservation of energy is written as the equality

$$\frac{dU}{dt} = -p\frac{dV}{dt} + \frac{dQ}{dt}.$$

The rate of heat supply/removal Q' is determined by the sum of the following factors:

- convective transfer across the boundaries of the volume under consideration Q'_c (or, Q'_e),

$$Q'_c = \begin{cases} c_\upsilon m'_r T_c, & \text{if } m'_r \geq 0; \\ c_\upsilon m'_r T_r, & \text{if } m'_r < 0; \end{cases} \qquad Q'_e = \begin{cases} c_\upsilon m'_r T_r, & \text{if } m'_r \geq 0; \\ c_\upsilon m'_r T_e, & \text{if } m'_r < 0; \end{cases}$$

- exchange of heat with the external environment Q'_{in} (or, Q'_{out}).

$$Q'_{in} = \alpha_e S_e (T_{\max} - T_e), \quad Q'_{out} = \alpha_c S_c (T_c - T_{\min});$$

here is the surface area of the heater

$$S_e = \frac{\pi d_2^2}{4} + L_e \pi d_2.$$

- thermal equivalent of the operation of an electric generator Q'_{gen},

$$Q'_{gen} = D_p \left(\frac{dx_p}{dt} \right)^2; \tag{11}$$

- thermal equivalent of the work of pushing gas through the regenerator $Q'_{r,c}$ (or, $Q'_{r,e}$),

$$Q'_{r,c} = \begin{cases} \dfrac{p_c - p_e}{\rho_r} m'_r, & \text{if } m'_r \geq 0; \\ 0, & \text{if } m'_r < 0; \end{cases} \qquad Q'_{r,e} = \begin{cases} 0, & \text{if } m'_r \geq 0; \\ \dfrac{p_c - p_e}{\rho_r} m'_r, & \text{if } m'_r < 0. \end{cases} \tag{12}$$

Thermal powers $Q'_{r,c}$ and $Q'_{r,e}$ always have a positive sign; if the gas flows from left to right, then the pushing work is performed by the coolant gas; if the gas flows in the opposite direction, then it is the heater gas. The rates of change in the volumes of the cooler and heater are equal

$$\frac{dV_c}{dt} = A_p \left(\frac{dx_d}{dt} - \frac{dx_p}{dt} \right), \qquad \frac{dV_e}{dt} = A_d \frac{dx_d}{dt}.$$

Then, from the law of conservation of energy, the rates of temperature changes T_c and T_e are determined,

$$c_\upsilon m_c \frac{dT_c}{dt} = -c_\upsilon T_c \frac{dm_c}{dt} - p_c A_p \left(\frac{dx_d}{dt} - \frac{dx_p}{dt} \right) - Q'_{out} - Q'_c - Q'_{gen} - Q'_{r,c},$$

$$c_\upsilon m_e \frac{dT_e}{dt} = -c_\upsilon T_e \frac{dm_e}{dt} - p_e A_d \frac{dx_d}{dt} + Q'_{in} + Q'_e - Q'_{r,e}.$$

Using equalities (4) allows the temperature equations to be written in a convenient form:

$$\frac{dT_c}{dt} = \frac{T_c}{m_c} m'_r - \frac{p_c A_p}{c_\upsilon m_c} \left(\frac{dx_d}{dt} - \frac{dx_p}{dt} \right) - \frac{Q'_{out} + Q'_{gen} + Q'_{r,c} + Q'_c}{c_\upsilon m_c},$$

$$\frac{dT_e}{dt} = -\frac{T_e}{m_e} m'_r - \frac{p_e A_d}{c_\upsilon m_e} \frac{dx_d}{dt} + \frac{Q'_{in} + Q'_e - Q'_{r,e}}{c_\upsilon m_e}.$$

Here, the first terms on the right sides of the equalities have the same structure, so they can be combined with convective heat sources. After simple transformations, the final forms of the equations for temperatures are obtained:

$$\frac{dT_c}{dt} = -\frac{p_c A_p}{c_\upsilon m_c} \left(\frac{dx_d}{dt} - \frac{dx_p}{dt} \right) - \frac{Q'_{out} + Q'_{gen} + Q'_{r,c}}{c_\upsilon m_c} + \tilde{Q}'_c, \tag{13}$$

$$\frac{dT_e}{dt} = -\frac{p_e A_d}{c_\upsilon m_e} \frac{dx_d}{dt} + \frac{Q'_{in} - Q'_{r,e}}{c_\upsilon m_e} + \tilde{Q}'_e,$$

$$\tilde{Q}'_c = \begin{cases} 0, & \text{if } m'_r \geq 0; \\ \dfrac{T_c - T_r}{m_c} m'_r, & \text{if } m'_r < 0. \end{cases} \qquad \tilde{Q}'_e = \begin{cases} \dfrac{T_r - T_e}{m_e} m'_r, & \text{if } m'_r \geq 0; \\ 0, & \text{if } m'_r < 0. \end{cases}$$

The inclusion of thermal powers (11) and (12) explicitly in the temperature equations (13) makes it possible to more accurately determine the temperature in the cooler and heater.

3. Modeling tools, construction of computational grid and verification of model accuracy and adequacy

The solution of equations (1), (2), (5), (9) and the system of equations (13) was carried out using the numerical Runge-Kutta method with second order accuracy [19]. The computational grid is taken from the same book. The program code for implementing the computational algorithm was written by one of the authors in C++ using the DevCpp 5.11 package.

The integration step is $\Delta t = 10^{-5}$ s; such a small value allows one to obtain reliable results with wide variations in engine parameters. The accuracy of the model was verified by decreasing the integration step Δt; the invariance of the results at different steps indicates the accuracy of the calculations [19]. The adequacy of the model was verified by checking the coincidence of the results with the results from work [15], obtained in the isothermal approximation.

4. Stirling machine simulation results

The analysis of its operation was carried out with the following set of input parameters:

- displacer mass $m_d = 0.1$ kg;
- heater length $L_e = 0.17$ m;
- spring stiffness $k_d = 500$ N/m;
- cross-sectional area of the displacer rod $A_{rod} = 0.01$ m^2;
- diameter $d_1 = 0.24$ m and displacer cross-sectional area $A_d = 0.045$ m^2;

– piston area $A_p = A_d - A_{rod} = 0.035$ m^2;
– piston mass $m_p = 0.2$ kg;
– damping coefficient (characterizes the reverse effect of an electric generator on a machine) $D_p = 8.0$ N·s/m;
– initial pressure $p_0 = 10^5$ Pa;
– working gas: adiabatic index (air) $\gamma = 1.4$, gas constant $R_g = 287$ J/(kg·K), heat capacity at constant volume $c_\upsilon = 710$ J/(kg·K);
– heat transfer coefficients $\alpha_c = \alpha_e = 250$ Вт/(м^2·K);
– heat exchange surface area of the cooler $S_c = 0.65$ m^2;
– heater heat exchange surface area $S_e = 0.19$ m^2;
– heat source temperature $T_{max} = 593$ K (320 °C);
– cooler (ambient) temperature $T_{min} = 293$ K (20 °C);
– distance $X_{e,0} = 0.26$ м;
– initial volumes $V_{e,0} = 1.46 \cdot 10^{-2}$ m^3, $V_{b,0} = 2.5 \cdot 10^5$ m^3, $V_{c,0} = 5.7 \cdot 10^{-3}$ m^3;
– neutral position of the displacer $x_{d,0} = 0.15$ m;
– geometric parameters of the regenerator $L_r = 0.18$ m, $d_r = 0.01$ m, $A_r = 7.85 \cdot 10^{-3}$ m^2; $V_r = 1.4 \cdot 10^{-3}$m^3;
– hydraulic parameters of the regenerator $K_r = 0.5$, $\zeta = 0.06$.

The volume of the buffer space is taken to be very large, $V_{b,0} = 2.5 \cdot 10^5$ m^3; in fact, it is excluded from consideration. High values of the heat transfer coefficients α_c and α_e suggest a rough account of the convective movement of the gas. But such movement is not considered in detail here, so as not to complicate the analysis of engine operation. The accepted value ζ corresponds to the weak porous structure of the regenerator; $\zeta = 0.03$ is realized in the free space of a channel with smooth walls [18].

The following was discovered during the simulation:
– the time it takes to reach a steady state of engine operation depends on the initial conditions for the differential equations;
– oscillations with very different frequencies occur in the system, so numerical integration of the equations must be carried out with a small-time step;
– under certain initial conditions, oscillations with very large amplitudes may occur in the first 0.01...0.1 s;
– with low spring stiffness k_d, the displacement of the displacer x_d may not correspond to the design of the engine and then the displacer rod may rest against the right or left wall. Sometimes this appears as a negative volume value V_e.

Results in Fig. 2–4 were obtained with initial conditions

$t = 0$: $x_p = 0$; $dx_p/dt = 0$; $x_d = x_{d,0}$; $dx_d/dt = 1$ m/s; $m'_r = 0$.

In addition to them, at the initial pressure p_0 and temperatures $T_e(t = 0) = T_{max}$, $T_c(t = 0) = T_{min}$, the gas masses in the cooler and displacer are equal

$$m_{c,0} = \frac{p_0 V_{c0}}{R_g T_c}, \quad m_{e,0} = \frac{p_0 V_{e0}}{R_g T_e}.$$

4.1. Methodology for calculating the generated power of electricity

Since the reverse influence of the electric current generator on the operation of the Stirling engine lies in the $D_p x'_p$ complex, it characterizes the production of electrical energy. The coefficient D_p depends on the properties of the generator [14]. The $D_p x'_p$ complex is the resistance force resulting from self-induction in the generator windings. Then the instantaneous electrical power is equal to

$$P = Q'_{gen} = D_p \left(x'_p\right)^2.$$

To assess the efficiency of the engine, the amplitude, or the average value over several periods of oscillation <*P*> in a steady state, is of interest. The positions of the displacer and piston (Fig. 2) are gradually established to a periodic oscillation mode with constant amplitudes. Clock frequency of oscillations in steady state ν = 12.3 Hz. The piston and the displacer perform synchronous oscillations; the presence of a noticeable phase shift between x_d and x_p is not detected. Such a small phase shift exists in the model [14], but not between pressure fluctuations in the heater and cooler.

Within one period of oscillation, the maximum speed of the piston is greater when moving to the right than in the opposite direction. Since the piston stroke is the same in both directions, the travel time is different. Due to the indicated difference in velocity amplitudes, the power graph (Fig. 3) in steady-state mode shows two maximum points $P_{max,1}$ = 427 W and $P_{max,2}$ = 598 W. Thus, the greatest engine power is developed when cold gas expands.

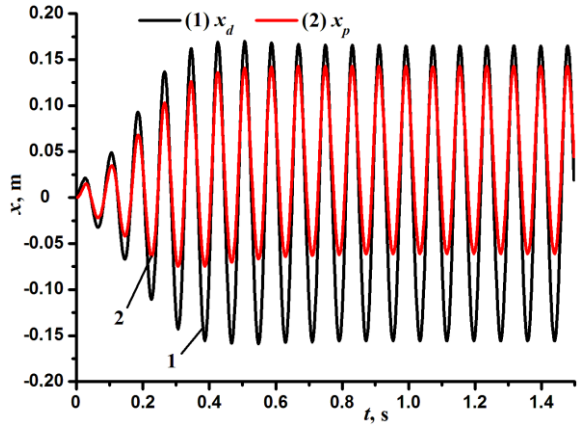

Fig. 2. Changes in the coordinates of the displacer x_d and piston x_p over time

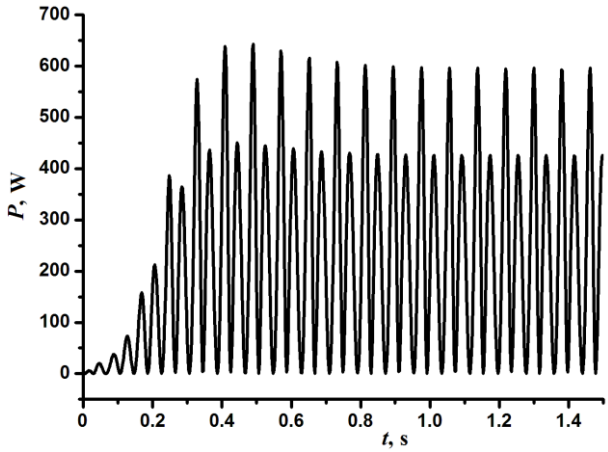

Fig. 3. Dependence of electrical power *P* on time *t*

The gas temperature in the heater T_e at certain moments of time exceeds T_{max} (Fig. 4). This occurs as a result of adiabatic compression of the gas under the influence of the inertia force of the displacer mass. But the average value <T_e> is always less than T_{max}. The gas temperature in the cooler T_c can increase both due to the incoming mass from the heater and as a result of adiabatic compression. In addition, T_c oscillations have a weakly expressed relaxation character, when the temperature increases faster than the decrease.

Temperature data <T_e> allows an approximate estimate of the electrical efficiency of the engine η. The temperature difference between the heater and the external temperature T_{max} is $\Delta T = T_{max} - \langle T_e \rangle$ = 84 K. Then the heat entering the engine is $Q'_{in} = \alpha_e S_e \Delta T$ = 4012 W. The net power produced is approximately <*P*> = 254 W, and then the efficiency is η = 0.063, or 6.3%.

It should be noted that the use of values with a temperature difference Q'_{in} (or Q'_{out}) is inconvenient, since the value ΔT is much smaller than the temperatures themselves, so they must be calculated with high accuracy.

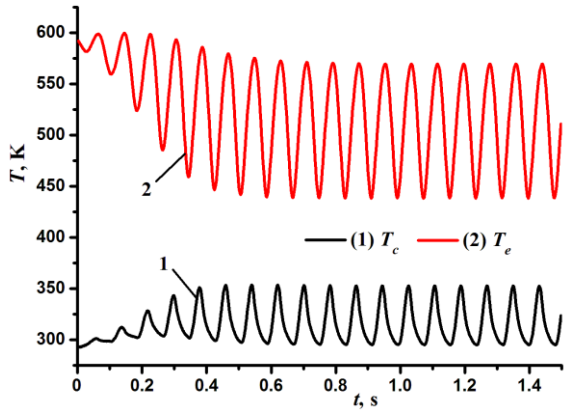

Fig. 4. Dependence of the temperature of the refrigerator T_c and the heater T_e on time t

Various thermodynamic cycles are realized in the heater and cooler; in the p-V coordinates one close to the Stirling cycle is observed, and in the cooler its almost mirror image is observed relative to the vertical axis (Fig. 5).

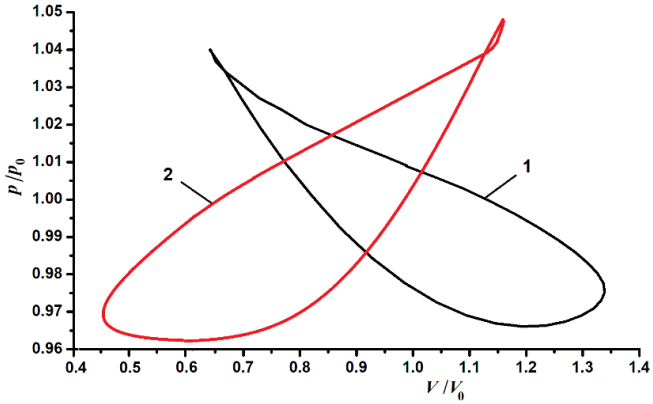

Fig. 5. Image in p-V coordinates of cycles in the heater (line 1) and cooler (line 2) in steady-state engine operation

A special feature of them is the presence of a small loop in the upper part of the figure; in addition, line 1 is not a Stirling cycle, since a decrease in pressure corresponds to an increase in volume. An increase in the hydraulic resistance coefficient K_r leads to a decrease in engine efficiency η (Fig. 6) and average power <P> (Fig. 7), the opposite phenomenon is observed depending on D_p.

The power of heat supplied to the engine Q'_{in} decreases at low K_r, and the observed increase in <P> means a more efficient conversion of heat into mechanical work. However, at low values of K_r, excessively large displacements of the displacer may be observed due to low spring stiffness k_d or small volume V_e, which do not correspond to the engine design. As the damping coefficient D_p increases, the pressure in the heater and cooler, as well as the difference between them, increases. This is explained by an increase in resistance to the movement of the piston, which leads to more mechanical work and the production of electrical power P.

In this regard, it would seem that the coefficient of hydraulic resistance K_r should have the same effect, but here the opposite phenomenon is observed (Fig. 7) the power <P> drops. The reason for this is a reduction in the exchange of heat and mass between the heater and cooler, which is fundamentally necessary in the Stirling cycle. An increase in engine power and efficiency can also be achieved by increasing the rigidity of the displacer spring, and at the same time this leads to an increase in the oscillation frequency (Fig. 8). Over the range of k_d changes indicated here, the power <P> increases from 64 to 251 W.

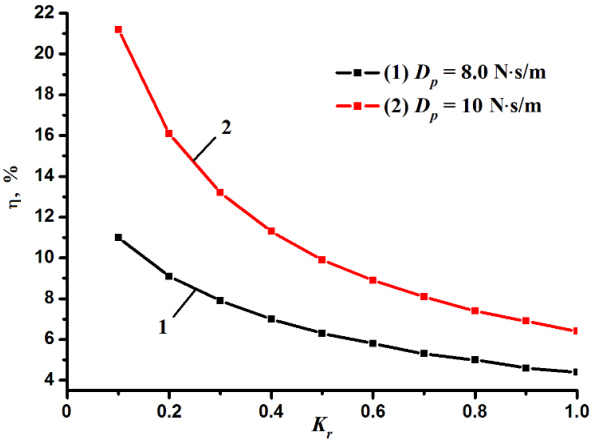

Fig. 6. Dependence of the electric efficiency of the engine η on the parameter K_r

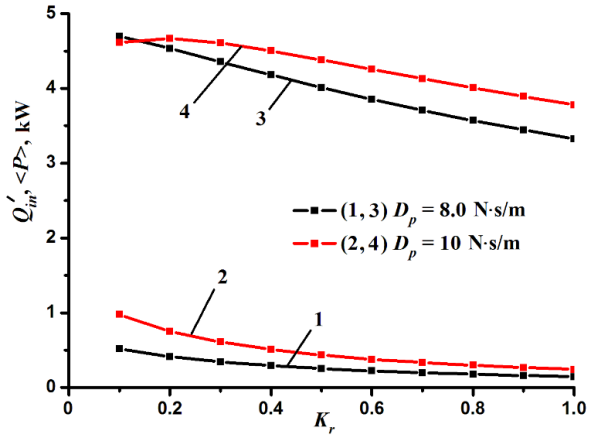

Fig. 7. Dependences of electric power <*P*> (lines 1, 2) and incoming heat Q'_{in} (lines 3, 4) on the K_r parameter

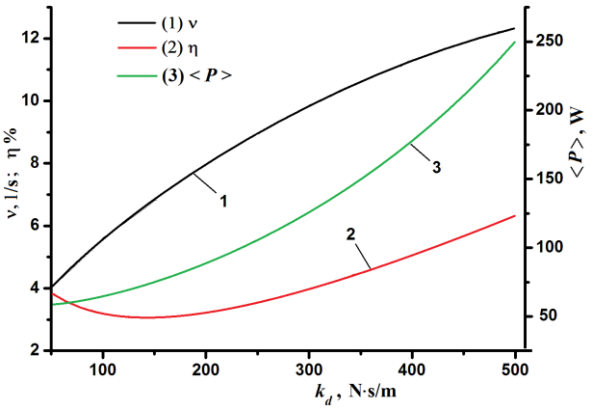

Fig. 8. Changes in frequency, efficiency and power when spring stiffness changes; K_r = 0.5, D_p = 8.0 N·s/m

The above results indicate the existence of an optimal operating mode for the Stirling engine depending on the spring stiffness, the hydraulic resistance of the regenerator, the connected electrical load and the geometric characteristics of the heater. The optimization procedure necessary in this case was not carried out; this is a separate and complex task due to the presence of a large number of parameters.

Here, the increase in efficiency η and power P depending on the load parameter k_d deserves special attention. Obviously, an unlimited increase in k_d will ultimately lead to the engine stopping. This means that the functions η(k_d) and P(k_d) must have a maximum point.

5. Comparison with the isothermal model [15]

Now temperatures $T_c = T_{\min}$, $T_e = T_{\max}$, equations (1.13) are not considered. In the isothermal approximation, the efficiency calculation is performed based on the value of the total engine power Pm (or the rate of production of mechanical work), it is equal to

$$P_m = \left|(p_c - p_e)\frac{dV_c}{dt}\right| + \left|(p_e - p_0)\frac{dV_e}{dt}\right| = \left|(p_c - p_e)A_p\left(\frac{dx_d}{dt} - \frac{dx_p}{dt}\right)\right| + \left|(p_e - p_0)A_d\frac{dx_d}{dt}\right|.$$

The necessity of the module sign is explained by the fact that useful work is performed both during expansion and compression of gas in volumes. The engine efficiency η was determined by the average values of power $\langle P \rangle$ and $\langle P_m \rangle$:

$$\eta = \frac{\langle P \rangle}{\langle P_m \rangle}.$$

The initial physical parameters remain the same as those used to construct Figures 6 and 7. Changing the resistance coefficient K_r from 0.1 to 0.9 does not change the efficiency, but the power is constantly reduced. And this result does not depend on the generator electrical load characteristic D_p. The obtained data are placed in Table 1.

Table 1. Dependence of average electrical power on the resistance coefficient K_r

D_p = 8 N·s/m									
K_r	0.1	0.2	0.3	0.4	0.5	0.6	0.7	0.8	0.9
η	17 % (for all K_r)								
$\langle P \rangle$, W	28	21	16	13	10	9	7	6	5
D_p = 10 N·s/m									
η	19 % (for all K_r)								
$\langle P \rangle$, W	53	40	31	24	20	17	14	12	10

It is also worth paying attention to the decrease $\langle P \rangle$ when switching to an isothermal model (power in Table 1 is measured in watts), but at the same time the efficiency increases. The constancy of the efficiency η found here is another distinctive feature of the isothermal model. It is generally accepted that friction always reduces the efficiency of the engine, but this is not observed in Table 1. Apparently, this is a shortcoming of the isothermal approximation.

6. Conclusion

Simulation of the Stirling engine showed a strong dependence of the results (temperatures in the heater and cooler, power and frequency) on the geometric and physical properties of the regenerator and the amount of work generated by the electric generator. In this case, the engine power increases with a decrease in the coefficient of hydraulic resistance in the regenerator and an increase in the load of the electric generator. An increase in power is also observed with an increase in the spring stiffness of the displacer, leading to an increase in the oscillation frequency. It was also found that the greatest power is observed in the absence of a phase shift between the oscillations of the displacer and the piston. The motor cannot run when the phase shift gets close to π. Increasing the stiffness of the displacer spring also leads to an increase in oscillation frequency, power and efficiency. Thermodynamic processes according to the Stirling cycle occur in the heater; in the cooler, a cycle is implemented that is close to mirror reflection relative to the pressure axis in *p-V* coordinates.

Comparison with an earlier isothermal model showed the following:

1) taking into account the change in temperature (in contrast to the isothermal model) in the engine leads to an increase in its power (for example, approximately 8.9 times with a spring stiffness of k_d = 500 N/m and D_p = 8 N·s/m);

2) but at the same time the efficiency of the engine increases for example, approximately 2.74 times with a spring stiffness of k_d = 500 N/m and D_p = 8 N·s/m);

3) in the isothermal approximation, the efficiency can remain constant with an increase in the hydraulic resistance of the regenerator K_r from 0.1 to 0.9, and this result does not depend on the damping coefficient D_p.

The obtained data are the result of calculations (simulation) under the specified simulation conditions and will be further analyzed for compliance with experimental data under similar operating conditions of the Stirling engine.

Notation

A_d – the cross-sectional area of the displace, m^2;
A_p – the cross-sectional area of the working piston, m^2;
A_{rod} – the cross-sectional area of the rod (displacer), m^2;
A_r, L_r – cross-sectional area and length of the regenerator, m^2 and m;
D_p – the coefficient characterizing the electric generator, N·s/m;
d_r – the height of the working section of the regenerator, m;
d_1 – the diameter of the piston and displacer, m;
d_2 – diameter of the heater and cooler, m;
k_d – spring stiffness coefficient, N/m;
m_c – the mass of gas in the cooler, kg;
m_e – the mass of gas in the heater, kg;
m_r, m'_r – mass and mass flow rate of gas in the regenerator, kg and kg/s;
P – electric power of the generator, W;
p_b, V_b – pressure and volume of buffer space, Pa and m^3;
p_0 – initial and external pressure, Pa;
Q'_{in} and Q'_{out} – heat input and output power in the engine, W;
$Q'_{r,c}$ and $Q'_{r,e}$ – thermal equivalents of the work of pushing gas through the regenerator, W;
Q'_c and Q'_e – thermal capacities of convective transfer across the boundaries of the cooler and heater, W;
R_g – gas constant, J/(kg·K);
$T_{\min}$, $T_{\max}$ – minimum and maximum temperature, K;
t – time, s;
V_c, p_c and T_c – volume, m^3, pressure, Pa, and gas temperature, K, in the cooler;
V_e, p_e and T_e – volume, m^3, pressure, Pa, and gas temperature, K, in the heater;
V_r, p_r and T_r – volume, m^3, pressure, Pa, and gas temperature, K, in the regenerator;
x_d, x_p – the coordinates of the displacer and piston, m;
u – gas velocity in the regenerator, m/s;
α_c, α_e – heat transfer coefficients in the cooler and heater, W/(m^2·K);
γ – adiabatic index;
η – electrical efficiency;
ρ_r – gas density in the regenerator, kg/m^3;
ν – the oscillation frequency of the piston and the displacer, s^{-1};
ζ, K_r – hydraulic resistance coefficients.

Subscripts: *c* – compression; *e* – expansion; *b* – buffer; *d* – displacer; *gen* – generator; *in* – inlet; *out* – output; *p* – piston; *r* – regenerator; *g* – gas.

Conflict of interest statement
The authors declare that they have no conflict of interest in relation to this research, whether financial, personal, authorship or otherwise, that could affect the research and its results presented in this paper.

CRediT author statement
Sabdenov K.O.: Conceptualization, Methodology, Writing-Review & Editing; **Erzada, M.:** Original Draft, Visualization, Software; **Zholdybaeva G.T.:** Conceptualization, Methodology.
The final manuscript was read and approved by all authors.

References

1 Ruihua Chen, Weicong Xu , Shuai Deng, Ruikai Zha, Siyoung Q. Choi, Li Zhao. (2023) Towards the Carnot efficiency with a novel electrochemical heat engine based on the Carnot cycle: Thermodynamic considerations. *Energy*, 284, 128577. DOI: 10.1016/j.energy.2023.128577.

2 Xu W, Deng S, Zhao L, Zhang Y, Li S. (2019) Performance analysis on novel thermodynamic cycle under the guidance of 3D construction method. *Applied Energy*, 250, 478 – 492. DOI: 10.1016/j.apenergy.2019.05.081.

3 Sabdenov K.O. (2021) The Thermodynamic Brayton Cycle with a Reversible Chemical Reaction. *Technical Physics,* 66, 1275 – 1283. Available at: https://link.springer.com/article/10.1134/S1063784221090164.

3 Sabdenov K. (2023) The Thermodynamics Cycles with a Reversible Chemical Reaction. *Americ. Journ. Mod. Phys.* (*AJMP*), 12, 2, 14 – 20. Available at: http://ajmp.org/article/10.11648/j.ajmp.20231202.11

4 Walker G. (1973) *Stirling-cycle machines*. Clarendon Press, Oxford, 156. Available at: https://www.amazon.com/Stirling-Cycle-Machines-Graham-Walker/dp/0198561121.

6 Reader G.T., Hooper Ch. (1982) *Stirling engines*, 424. Spon Press. Available at: https://www.abebooks.co.uk/9780419124009/Stirling-Engines-Reader-G.T-Hooper-0419124004/plp

7 Valenti G., Campanari S., Silva P., Ravida A., Macchi E., Bischi A. (2015) On-off cyclic testing of a micro-cogeneration Stirling unit. *Energy Procedia*, 75, 1197–1201. Available at: https://www.researchgate.net/publication/281373930_On-off_Cyclic_Testing_of_a_Micro-cogeneration_Stirling_Unit

8 Sabdenov K.O., Erzada M., Suleimenov A.T. (2019) The Possibility of Converting Energy in Space with the Aid of a Chain Heat Machine Operating on Methane and Nitrogen. *Journ. Eng. Phys. Therm*., 92, 3, 574-584. Available at: https://link.springer.com/article/10.1007/s10891-019-01965-z#citeas

9 Konyukhov G.V., Bukharov A.V., Konyukhov V.G. (2020) On the Problem of Rejection of Low-Potential Heat from High-Power Space Systems. *Journ. Eng. Phys. Therm.,* 93, 16–27. Available at: https://doi.org/10.1007/s10891-020-02086-8

10 Vikulov A.G., Morzhukhina A.V. (2021) Controlling the Power of the Internal Heat Sources of Space Vehicles. *Jour. Eng. Phys. Therm.,* 94, 1101–1109. DOI: 10.1007/s10891-021-02390-x.

11 Xu W, Deng S, Zhao L, Zhang Y, Li S. (2019) Performance analysis on novel thermodynamic cycle under the guidance of 3D construction method. *Applied Energy*, 250, 478-492. DOI: 10.1016/j.apenergy.2019.05.081.

12 Jenkins N., Ekanayake J.B., and Strbac G. (2010) *Distributed Generation*. The Institution of Engineering and Technology, London. Available at: https://web.nit.ac.ir/~shahabi.m/M.Sc%20and%20PhD%20materials/DGs%20and%20MicroGrids%20Course/Books/Distributed%20Generation%20by%20N.Jenkins%20IET%20press/Distributed.pdf.

13 Dulau L. I., Abrudean M., Bica D. (2014) Effects of Distributed Generation on Electric Power Systems. *Procedia Technology*, 12, 681–686. Available at: https://www.researchgate.net/publication/270916389_Effects_of_Distributed

14 Langlois, Justin L.R. (2006) Dynamic computer model of a Stirling space nuclear power system. *Trident Scholar project report no. 345*. Annapolis, US Naval Academy. Available at: https://www.semanticscholar.org/paper/Dynamic-Computer-Model-of-a-Stirling-Space-NuclearLanglois/0e513dee372464b9d6807efb9717e934af1c4df1

15 Sabdenov K.O. (2024) A simple model of a Stirling machine (engine) with a free working piston. *Journ. Eng. Phys. Therm.,* 97, 4. P. 1034-1041. DOI: 10.1007/s10891-024-02974-3.

16 Zhiwen Dai, Chenglong Wang, Dalin Zhang, Wenxi Tian, Suizheng Qiu, G.H. Su**.** (2021) Design and analysis of a free-piston Stirling engine for space nuclear power reactor. *Nucl. Eng. Techn*., 53, 2, 637–646. DOI:10.1016/j.net.2020.07.011.

17 Fr. Catapano, C. Perozziello, B. M. Vaglieco. (2021) Heat transfer of a Stirling engine for waste heat recovery application from internal combustion engines. *Appl. Therm. Eng*., 198, 5, 117492. DOI:10.1016/j.applthermaleng.2021.117492.

18 Ukhin B.V., Gusev A. A. (2010) *Hydraulics*. Moscow, 432. Available at: https://www.ibooks.ru/products/360607? Category id=12968 [in Russian]

19 Kalitkin N.N. (2011) *Numerical methods*. Moscow, 592. Available at: https://bhv.ru/wp-content/uploads/wpallimport/ filespdfk i/view_1768_978-5-9775-5000.pdf?srsltid=AfmBOoq6JfthMR60no1rnchXvS2xar [in Russian]

AUTHORS' INFORMATION

Sabdenov, K.O. - Doctor of Phys.- Math. Sciences, Professor, Electrical Engineering Department, Transport and Energy Faculty, L.N. Gumilyov Eurasian National University, Astana, Kazakhstan; ORCID: 0009-0008-4733-6667; sabdenovko@yandex.kz

Erzada, M. - Doctor (Eng.), Associate Professor, Electrical Engineering Department, Transport and Energy Faculty, L.N. Gumilyov Eurasian National University, Astana, Kazakhstan; ORCID: 0000-0002-3943-651X; mayira76@yahoo.co.jp

Zholdybaeva G.T. – Master (Eng.), Teacher, Mathematics Department, M. Saparbaev South Kazakhstan Humanitarian Institute, Shymkent, Kazakhstan; ORCID: 0009-0008-4733-6667; gulnur_rashid@mail.ru